

Effect of Hydrophobic Particles in a Gas Diffusion Electrode on Cell Performance in Polymer Electrolyte Membrane Fuel Cells

In-Tae Kim¹, Jae-Young Lee², Hyung-Ryul Rim², Hong-Ki Lee², Joongpyo Shim^{3,*}

¹Graduate School of Science and Engineering, Yamaguchi University, Ube, 755-8611, Japan

²Fuel Cell Regional Innovation Center, Woosuk University, Jeonbuk, 565-701, Korea

³Department of Nano & Chemical Engineering, Kunsan National University, Jeonbuk, 573-701, Korea

*E-mail: jpshim@kunsan.ac.kr

Received: 21 August 2015 / Accepted: 16 September 2015 / Published: 30 September 2015

The relationship between cell performance and the hydrophobic properties of a catalytic layer containing hydrophobic particles in a gas diffusion electrode for a polymer electrolyte membrane fuel cell was investigated. The hydrophobic particles, prepared from carbon black and polytetrafluoroethylene dispersion, were added to a catalytic layer to form a gas diffusion network by enhancing the hydrophobic property of the catalytic layer. The cell performance increased as the catalytic layer became more hydrophobic. A more hydrophobic catalytic layer reduced blockage of the gas diffusion path that water, reaction product, caused. Water was produced by the electrochemical reaction of the reactant gases at the catalytic layer. The hydrophobic property of the catalytic layer was more important at the high current density region compared with the low current density region. A three-layered electrode system with a test layer and catalytic layer were used to investigate the flux of humidified gas through the catalytic layer. The hydrophobic nature of the test layer determined by the amount of hydrophobic particles in the catalytic layer influenced the gas flux and changed the cell performance.

Keywords: PEMFC, gas diffusion electrode, hydrophobic particle, cell performance, gas flux

1. INTRODUCTION

Fuel cells are clean power sources that can contribute to the solution of many current environmental problems through their high energy conversion efficiencies and low CO emission compared with conventional internal combustion power generation. Several types of fuel cells have been developed, including polymer electrolyte membrane fuel cells (PEMFC) and direct alcohol fuel cells operating at ambient temperatures. Fuel cells have become the power sources for electric vehicles (EV) and portable devices. To obtain high cell performance with a reduced Pt loading in the electrode, many researchers have proposed various preparation methods for gas diffusion electrodes (GDEs),

catalyst layers (CLs) and catalysts [1-10]. Yano *et al.* has developed a nano-capsule method using various types of carbon black to enhance the efficiency of Pt loading, mass activity (MA), cyclability and start-stop durability to facilitate high Pt utilization (U_{Pt}) [11-19]. Also, Taylor *et al.* reported that using electrochemical catalyzed (ECC) techniques, GDEs for PEMFC application were prepared [20,21]. They prepared electrodes containing 0.05 mg-Pt/cm^2 , in which the platinum catalyst was in regions of the electrode that were in ionic contact with the polymer electrolyte and electronic contact with the carbon support.

High U_{Pt} and high MA for catalysts are important in terms of cost-efficiency and cell performance. GDEs need to have high MA and high U_{Pt} through the uniformly supplied reactant gases and elimination of water molecules that were formed on the CL. Many researchers for gas diffusion layer (GDL) have also investigated improvement of cell performance by increasing gas permeability and electrochemical surface area (ECSA) [22-28]. In particular, the effect of the microstructure and hydrophobic properties of porous GDEs for low-temperature fuel cell operation, e.g. phosphoric acid fuel cell (PAFC), alkaline fuel cell (AFC) and PEMFC have been reported [10, 29-36]. Wilson and Gottesfeld reported that although polytetrafluoroethylene (PTFE) was effective as a binder and could increase the diffusibility of gas to impart hydrophobic properties to the gas diffusion region of the electrode, PTFE did not impact catalytic activity [7]. Sakai *et al.* observed that the oxygen permeability through the hydrated polymer electrolyte was higher than through PTFE particles [37]. Uchida *et al.* investigated the effect of a perfluorosulfonate ionomer and a PTFE-loaded carbon in the CL in PEMFCs using electrochemical techniques and a mercury pore sizer [38]. Uchida *et al.* observed that the quantity of PTFE in the electrode greatly influenced the performance of PEMFC at high current densities due to its gas diffusion capability.

In this paper, the effect of hydrophobic materials and humidified gas flux in PEMFC electrodes were investigated. Hydrophobic particles, HFP, were prepared by mixing PTFE and carbon black. Water management in PEMFC electrodes is an important factor in cell operation. The GDL and the CL of PEMFC electrodes must have adequate hydrophobic properties to remove water produced by the electrochemical reaction. The hydrophobic properties of an electrode can be properly controlled by the amount of HFP present.

2. EXPERIMENTAL

PTFE-loaded carbon black (an HFP) was prepared by mixing carbon black (Vulcan XC-72, Cabot Co.), PTFE dispersion (60 %, DuPont Co.), and a surfactant (Triton X-100, Aldrich Co.) in water. The mixed powder (denoted $x\text{HFP}$), which was composed $x \text{ wt\%}$ PTFE and $(100-x) \text{ wt\%}$ carbon was dried at $60 \text{ }^\circ\text{C}$ for 12 h. Then, the mixture was heat-treated at $340 \text{ }^\circ\text{C}$ for 1 h in air to complete the preparation of $x\text{HFP}$ and remove the surfactant. Heat-treated $x\text{HFP}$ was homogeneously pulverized by a mechanical mill.

The surface area and pore size distribution of HFP were measured by a BET (Brunauer-Emmett-Teller) analyzer (ASAP 2020, Micromeritics). The contact angles of HFP and CL containing HFP were measured by a contact angle analyzer (Phoenix, Pico). HFP was pelletized to a size of 2 cm diameter and 2 mm thickness at a pressure of 5 MPa for contact angle measurements.

A Nafion 115 membrane (DuPont Co.) used as a polymer electrolyte was pretreated by heating first in pure water, and second in a 5% H₂O₂ solution at 70 – 80 °C for 1 h to remove organic impurities. Then, this membrane was treated with 0.5 M H₂SO₄ at 70 – 80 °C for 1 h. The membrane was finally washed in boiling pure water to remove H₂SO₄.

The GDE was prepared as follows: The catalyst ink was prepared by mixing catalyst powder (10% Pt/C, DeNora), HFP, Nafion solution (5% solution, DE521, DuPont) and solvent (mixture of water and isopropyl alcohol). The mixed catalyst ink was painted on a wet-proofed carbon cloth (ELAT, NuVant) until the desired amount of Pt was loaded. The coated carbon cloth was then dried at 60 °C in air to remove the solvent in the catalyst ink. The resulting GDE was hot-pressed with pretreated Nafion 115 at a pressure of 1500 psi and a temperature of 100 °C for 2 min to sandwich the membrane electrode assembly (MEA). Three-layered electrode systems with a test layer and CL were prepared to measure the gas flux versus the content of HFP. Three-layered electrodes consist of a GDL, test layer and CL. A test layer was prepared by painting the mixture of carbon, HFP and Nafion solution on GDL, which is similar to the CL without the Pt catalyst, and then CL was coated on the test layer. This three-layered electrode serving as the cathode was hot-pressed with a Nafion 115 membrane and a normal GDE as anode to make the MEA. This test layer is similar to the micro porous layer (MPL) on the GDL, but it is different in that it contains a polymer electrolyte in layer.

Single cell is assembled with MEA, gaskets, a Au-coated copper plate current collector and two graphite plates with ribbed channels for the distribution of reactant gas behind the porous GDE. The MEA is located between two graphite plates like a sandwich. A copper plate as a current collector was located behind the graphite plate. The active size of the graphite plate was 4 cm². The test station for the single cell performance measurement was composed of a temperature controller, humidification chamber, flowmeter, back pressure regulator and electronic loader (Daegil Electronics, EP-1200). Humidified hydrogen (H₂) and oxygen (O₂) gas was supplied to the anode and cathode, respectively. The utilization of reactant gases was 50 % for H₂ and O₂. These gases were humidified at 100 % relative humidity (RH) by bubbling through a humidification chamber filled with water. For the electrochemical performance measurement, cells were maintained at 80 °C. H₂ and O₂ gases were supplied at 90 °C and 85 °C, respectively. The pressure of all supplied gases was 1 atm.

Before the test, MEA activation was carried out because the polymer electrolyte membrane was in a dry state when the cell was assembled. For MEA activation, the cell was operated at a constant current density of 500 mA/cm² for 12 h. After activation, cell performance measurements were conducted using these same conditions. The current-voltage (I-V) curves were recorded under steady-state operation condition after waiting 5 min. During the test of the three-layered electrode system, the gas flux (mole/cm²h) through the test layer was calculated from the current density.

3. RESULTS AND DISCUSSION

The humidified gases that pass through the GDL diffuse into the CL. If there is a gas diffusion network in the CL, the humidified gas can diffuse more easily into the catalytic site through the CL. Watanabe et al. proposed a new type electrode for phosphoric acid fuel cell that had hydrophilic Pt/C as the electrolyte network and PTFE-loaded carbon black as gas-supplying network in CL [30].

Watanabe's group demonstrated the possibility of designing an ideal electrode structure enabling 100% utilization of the catalyst clusters without polarization losses caused by mass transport with a high current density at the optimized structure. Also, they proposed a new concept for a high performance PEMFC using new preparation method for the GDE [39]. The new GDE preparation method included; (1) a new coating method for a homogeneous Nafion coating on the supported electrocatalysts, (2) heat treatment of the Nafion-coated electrocatalysts to prevent Nafion elution, and (3) a paste method for attaching the electrocatalyst particles to each other.

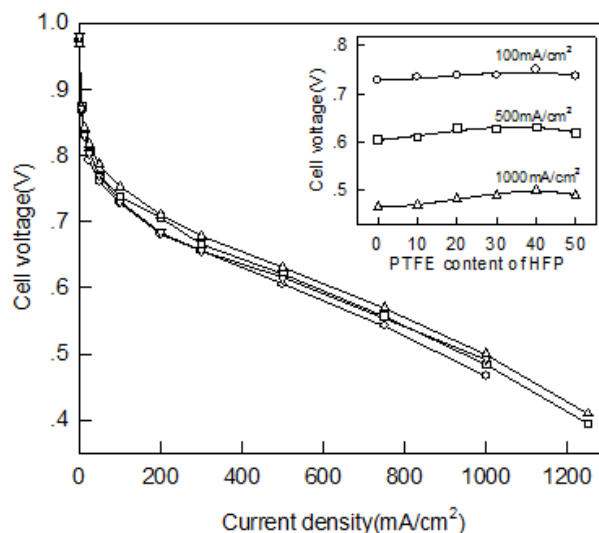


Figure 1. I-V curves of cells with CL containing HFP with different PTFE content. Pt/C : carbon : HFP = 5 : 4 : 1. PTFE content in HFP (○) 0%, (□) 20%, (△) 40%, (▽) 50%. Pt loading 0.3 mg-Pt/cm².

Fig. 1 shows the performance of a single cell with a CL containing HFP with different PTFE contents at both sides of the anode and cathode. The ratio of Pt/C : carbon : HFP was 5 : 4 : 1. The reason for the addition of more carbon was to maintain the ratio of Pt/C in the CL independent of the change in HFP content later. The cell performance increased as the hydrophobic properties of HFP increased (by increasing the PTFE content of HFP). The cell voltage difference at high current densities was greater than at low current density, as shown in the inset of Fig. 1. These results mean that the hydrophobic properties of the CL play a more important role at high current densities (the mass transfer control region) than at low current densities (the activation control region). When a fuel cell operates, water is produced in the CL by electrochemical reaction of the humidified reactant gases, H₂ and O₂, on the Pt catalysts. This water prevents reactant gases from diffusing to the catalytic site, especially the hydrophilic portion of the CL, by blocking the diffusion paths of the gases. Hence, the cell performance decreases because mass transport is reduced.

Watanabe *et al.* investigated the microstructure of the CL and the performance of a PTFE-bonded GDE for a phosphoric acid fuel cell having different PTFE contents using electrochemical techniques and a mercury pore sizer [29]. The CL consisted of two distinctive pore distributions with a

boundary of $\sim 0.1 \mu\text{m}$. The smaller pore (primary pore) was assigned to the space in-between the primary particles residing in their agglomerates and the larger pore (secondary pore) to the space in-between the agglomerates. Uchida *et al.* measured the specific pore volume distribution of the membrane electrode assembly with a polymer electrolyte and PTFE-C (PTFE-loaded carbon black) [38]. Uchida's group defined the pores with sizes $0.02 - 0.04 \mu\text{m}$ to be the primary pores and the pore with sizes $0.04 - 1.0 \mu\text{m}$ to be the secondary pores in the PEFC electrode.

Table 1. Physical properties of HFP and carbon black.

	BET (m^2/g)	Pore volume (cc/g)			Contact angle ($^\circ$)	Contact angle* ($^\circ$)
		Total	$>0.02\mu\text{m}$	$<0.02\mu\text{m}$		
Carbon black (0HFP)	235.6	0.957	0.811	0.146	94	159
10 HFP	96.5	0.415	0.289	0.126	147	150
20 HFP	74.6	0.345	0.235	0.109	155	148
30 HFP	65.1	0.331	0.245	0.086	160	146
40 HFP	52.5	0.243	0.186	0.062	164	144
50 HFP	49.5	0.198	0.138	0.060	167	144

* Contact angle of catalyst layer with HFP (Pt/C : carbon : HFP = 5 : 4 : 1)

The pore-size distribution of HFP was measured by the BET method (Fig. 2).

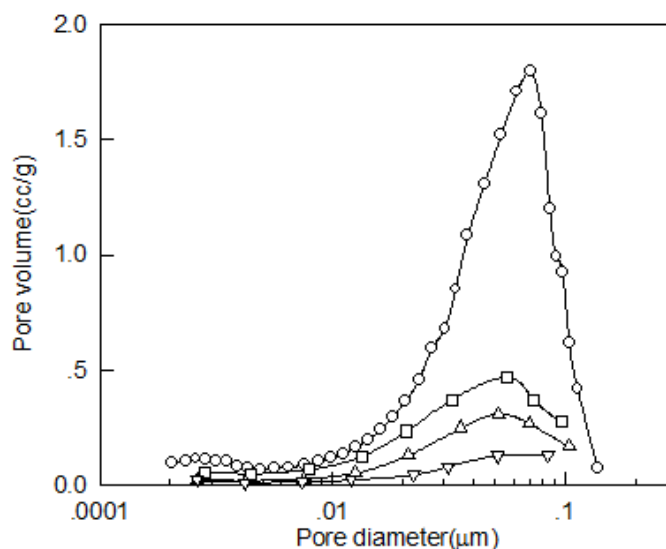


Figure 2. Pore size distributions of carbon black and HFP. (○) carbon black (Vulcan XC-72), (□) 10HFP, (Δ) 30HFP, (▽) 50HFP.

Most pores had a size in the $0.02 - 0.1 \mu\text{m}$ range. The pore volume decreased considerably as PTFE was loaded on the carbon. Because the particle size of carbon black (Vulcan XC-72) was $0.03 \mu\text{m}$ [40], pores in the range of $0.02 - 0.1 \mu\text{m}$ were made from space between agglomerates of carbon

black particles. Watanabe [29] classified pores ($> 0.02 \mu\text{m}$) and pores ($< 0.02 \mu\text{m}$) as macropores and micropores, respectively. Table 1 shows the BET surface area, pore volume, and contact angle of carbon black and HFP. Also, the surface area of HFP decreased considerably as the addition of PTFE progressed. The macropore volume decreased considerably with increasing PTFE content, but the micropore volume decreased slightly. This means that added PTFE particles block the macropores made by agglomerates of carbon black particles.

The contact angle of a powder is an important factor related to its hydrophobic property. Watanabe *et al.* measured the contact angle of 105% phosphoric acid at 190°C to examine the hydrophobic properties of prepared particles [41]. Watanabe's group observed that the contact angle of a GDL showed similar values regardless of the PTFE content in the layer. But, in this study, the contact angle of HFP for water at room temperature increased with increasing PTFE content. The results of this study were different than Watanabe's result because of the difference in solutions used.

It has been reported that a Nafion membrane is hydrated with liquid water within a few tens of seconds [42], whereas it takes much longer for this membrane to completely equilibrate with the aqueous vapor phase [43]. Zawodzinski *et al.* investigated contact angles measured on Nafion membranes to obtain some information on the hydrophilic property of the ionomer surface [44]. The water, which was supplied into the membrane and extracted out of the electrode, must diffuse through the CL of the fuel cell electrode. Therefore, the hydrophobic property of the CL is important in the polymer electrolyte membrane fuel cell. Table 1 shows the contact angle of CL on the PTFE content of HFP (Pt/C : carbon : HFP = 5 : 4 : 1). The contact angle of the CL decreased as the PTFE content of HFP increased. Because the surface area of HFP decreased as the PTFE content increased, the amount of the polymer electrolyte membrane on the surface of the electrode increased and the contact angle of the CL decreased by slight hydration of its membrane.

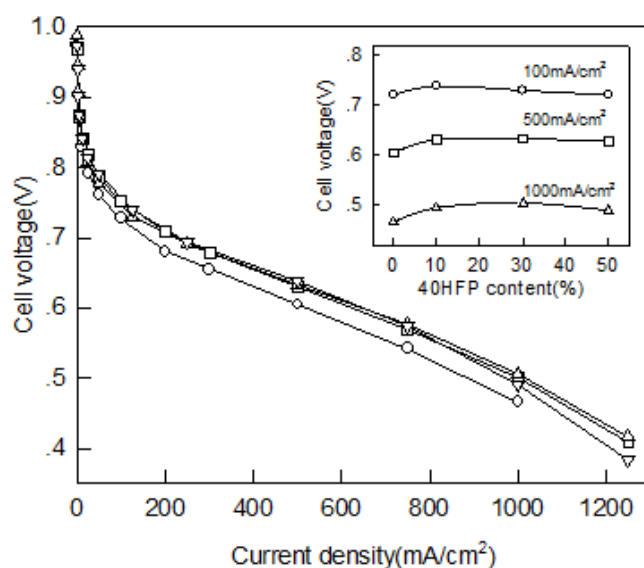


Figure 3. I-V curves of cell with CL containing different content of 40HFP. Pt/C : carbon : 40HFP = (○) 5 : 5 : 0, (□) 5 : 4 : 1, (Δ) 5 : 2 : 3, (▽) 5 : 0 : 5. Pt loading 0.2 mg-Pt/cm^2 .

40HFP in the CL showed the highest cell performance (Fig. 1). Fig. 3 shows the I-V curves with various contents of 40HFP in the CL. Cell performance increased with increasing 40HFP contents up to 30 %, then it decreased. The ratio of weight percent of PTFE to the total carbon amount at maximum performance was ca. 17%. Arico *et al.* observed that the best electrode was one containing PTFE for oxygen reduction on Nafion-coated dual-layered GDEs at 60 °C in 2.5 M H₂SO₄ [45]. This electrode showed that cell performance is influenced by the PTFE content in the CL.

The inset in Fig. 3 shows the variation of cell voltage at several current densities versus 40HFP content in the CL. At high current densities, in the region of mass transport, the difference in cell voltage was greater than at low current densities, the region of activation control. The results of this work suggest that the hydrophobic property of 40HFP improved the cell performance by enhancing gas diffusion. As shown in the schematic diagrams in Fig. 4 (a), the reactant gases may be limited to reach the Pt catalysts because the water produced blocks the gas channels in the CL. On the other hand, as shown in Fig. 4 (b), the reactant gases are able to more easily reach the Pt catalysts due to water removal by HFP in the CL. These differences affect the cell performance by improving the mass transfer of reactant gases, especially in the high current density region.

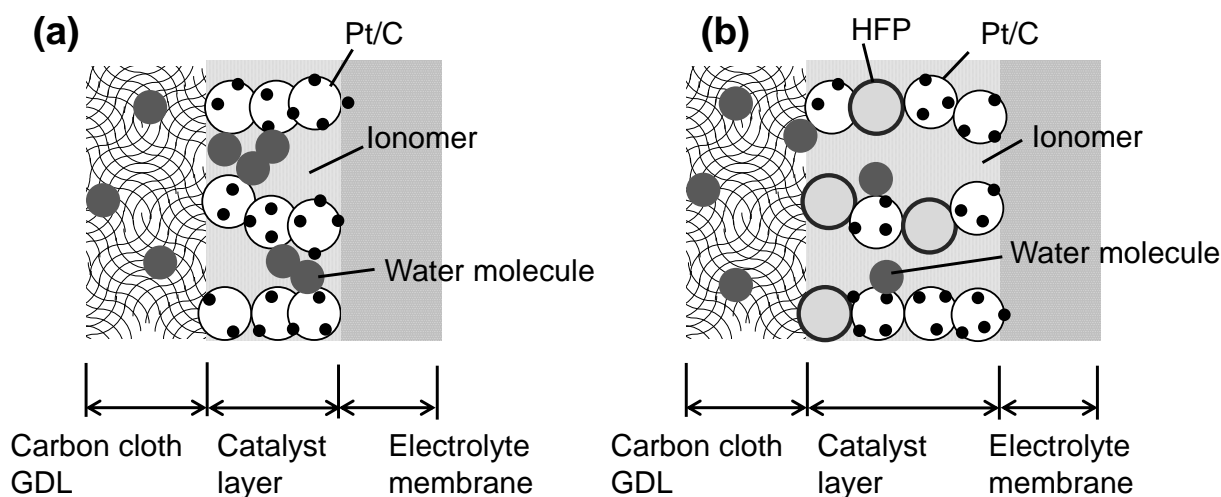


Figure 4. Schematic cross-sections of MEA with and without HFP (a) and 40HFP (b) in CL

Kenjo and Shim investigated the gas and electrolyte diffusivity using multilayered electrodes in AFC [36,46]. In this work, the test layer in the three-layered electrode system, which had a similar composition to the CL but no Pt catalyst, was used to indirectly measure gas flux through the layer with different hydrophobic properties. Humidified reactant gases passing through the GDL must penetrate through the test layer containing different amount of HFP to reach the CL. The diffusions of humidified gases were changed by the hydrophobic properties of the test layer. Therefore, variation of the humidified gas concentration and the water uptake of the polymer electrolyte membrane occurred in the CL, and then the cell performance was affected.

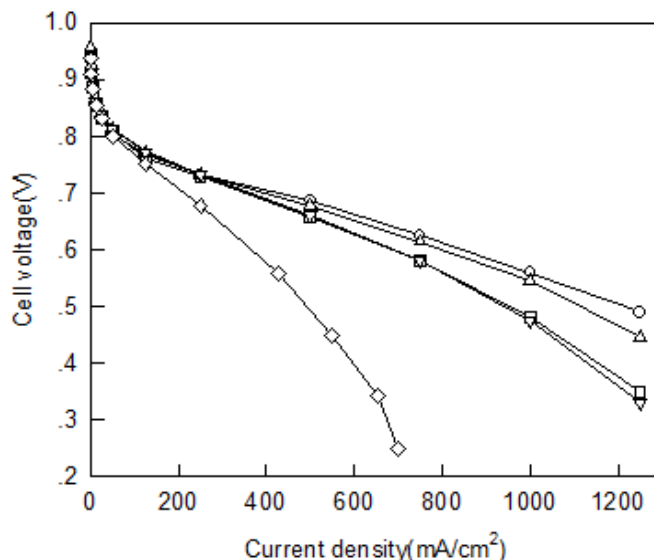


Figure 5. I-V curves of cells with three layered electrode containing different content of 40HFP content in test layer. 40HFP content (○) no test layer, (□) 0%, (Δ) 10%, (▽) 30%, (◇) 50%. Pt loading 0.38 mg-Pt/cm².

Fig. 5 shows the performance of the cell with and without the test layer. Cell with the test layer containing 10 % of 40HFP showed similar performance to that without the test layer. The rest of the electrode showed low performance. The cell with the test layer containing 50 % of 40HFP showed the lowest performance. The variation of porosity and hydrophobicity of the test layer determined by the content of HFP changed the flux of reactant gases through the test layer and led to the change in cell performance.

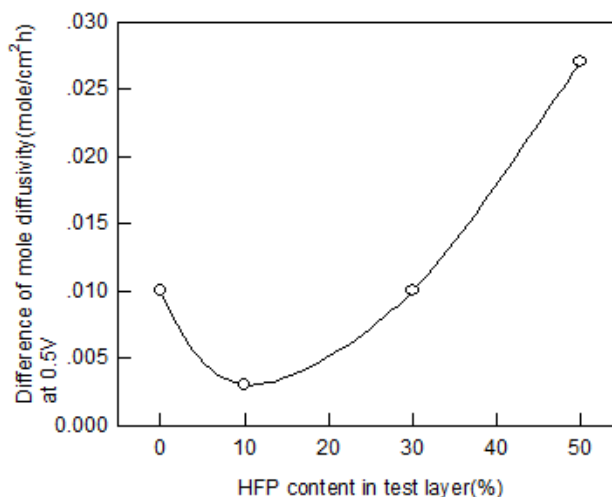


Figure 6. Difference of specific mole diffusivity through test layer with different content of 40HFP. Difference of specific mole diffusivity was calculated at 500mA/cm² comparing to cell without test layer.

The mole diffusivity of humidified gases can be determined from the polarization data of the electrode using the three-layered electrode system [36,46]. Since the test layers do not have catalytic activity, the humidified gas penetrating through these layers reacts in the CL.

Fig. 6 shows the difference of specific mole diffusivities for humidified gases that passed through the test layer compared with electrodes without the test layer. The specific mole diffusivity was calculated from the current density at 0.5 V, assuming that the reactant gas, which was diffused into the CL through the test layer, fully reacted on the high loading Pt catalysts in the CL. The test layer containing 10% of 40HFP showed the lowest mole diffusivity difference. In a fuel cell system (Fig. 3), the CL containing 30 % of 40HFP showed the highest cell performance but, in the three-layered electrode system, the cell with a test layer containing 10 % of 40HFP exhibited the highest mole diffusivity. We think that, in fuel cell systems, water is produced by the electrochemical reaction at the CL during cell operation. Some of the water produced diffuses into the electrolyte membrane via a concentration gradient, and the rest moves out through the GDL [47,48]. We consider that there was more water at the CL than at the test layer in the three-layered electrode system. If there is much water in the layer, the hydrophobic property of the layer may be important in order to make a path for the diffusion of gas. But, if there is little water, pore distribution is more important than the hydrophobic property because water doesn't block the path for gas in the layer. The difference of cell performance between fuel cell system (Fig. 3) and the three-layered electrode system (Fig. 5) may be due to how much water exists in the layer. Finally, the effect of HFP on the hydrophobic property of the CL was simply calculated by using a three-layered electrode system and monitored by the changes in cell performance.

4. CONCLUSIONS

By enhancing the hydrophobic property of CL, PTFE-loaded carbon black serving as the HFP was added to the CL in order to form a gas diffusion network. Even though the surface area of HFP decreased with the addition of PTFE, cells with a CL containing HFPs showed the highest performance at 30% of the HFP, which was *ca.* 17% of PTFE relative to the total quantity of materials in the CL. The mole diffusivity for humidified gases passing through the layer with HFPs was measured by using a three-layered electrode system that changed according to the content of HFPs in the layer. These results confirm that the diffusion of reactant gases through a CL can be enhanced by the introduction of hydrophobic property, especially the addition of HFPs.

ACKNOWLEDGEMENT

This work was financially supported by the Program of Regional Innovation Center at Woosuk University which was conducted by the Ministry of Knowledge Economy of the Korean Government.

References

1. S. Srinivasan, E.A. Ticianeli, C.R. Derouin, A. Redondo, *J. Power Sources*, 22 (1988) 359.
2. E.A. Ticianelli, C.R. Derouin, A. Redondo, S. Srinivasan, *J. Electrochem. Soc.*, 135 (1988) 2209.

3. M.S. Wilson, S. Gottesfeld, *J. Electrochem. Soc.*, 139 (1992) L28.
4. M.S. Wilson, U.S.P. 5,234,777(1993).
5. V.A. Paganin, E.A. Ticianelli, E.R. Gonzalez, *J. Appl. Electrochem.*, 26 (1996) 297.
6. D.R. de Sena, E.A. Ticianelli, E.R. Gonzalez, *J. Electroanal. Chem.*, 357 (1993) 225.
7. M.S. Wilson, S. Gottesfeld, *J. Appl. Electrochem.*, 22 (1992) 1.
8. K.D. Beard, M.T. Schaal, J.W. Van Zee, J.R. Monnier, *Applied Catalysis B: Environmental*, 72 (2007) 262.
9. R.S. Amin, A.A. Elzatahry, K.M. El-Khatib, M. E. Youssef, *Int. J. Electrochem. Sci.*, 6 (2011) 4572.
10. J. M. Song, H. Uchida, M. Watanabe, *Electrochemistry*, 73 (2005) 189.
11. H. Yano, M. Kataoka, H. Yamashita, H. Uchida, M. Watanabe, *Langmuir*, 23 (2007) 6438.
12. H. Yano, J. M. Song, H. Uchida, M. Watanabe, *J. Phys. Chem. C*, 112 (2008) 8372
13. K. Okaya, H. Yano, H. Uchida, M. Watanabe, *Appl. Mater. Interfaces*, 2 (2010) 888
14. H. Yano, T. Akiyama, P. Bele, H. Uchida, M. Watanabe, *Phys. Chem. Chem. Phys.*, 12 (2010) 3806
15. H. Yano, T. Akiyama, H. Uchida, M. Watanabe, *Energy Environ. Sci.*, 3 (2010) 1511
16. H. Uchida, H. Yano, M. Wakisaka, M. Watanabe, *Electrochemistry*, 79 (2011) 303
17. K. Okaya, H. Yano, K. Kakinuma, M. Watanabe, H. Uchida, *Appl. Mater. Interfaces*, 4 (2012) 6982
18. H. Yano, T. Akiyama, M. Watanabe, H. Uchida, *J. Electroanal. Chem.*, 688 (2013) 137
19. M. Uchida, Y.-C. Park, K. Kakinuma, H. Yano, D. A. Tryk, T. Kamino, H. Uchida, M. Watanabe, *Phys. Chem. Chem. Phys.*, 15 (2013) 11236
20. N.R.K. Vilambi, E.B. Anderson, E.J. Taylor, U.S.Pat. 5,084,144(1992).
21. E.J. Taylor, E.B. Anderson, N R.K. Vilambi, *J. Electrochem. Soc.*,139 (1992) L45.
22. L.R. Jordan, A.K. Shukla, T. Behrsing, N.R. Avery, B.C. Muddle, M. Forsyth, *J. Power Sources*, 86 (2000) 250.
23. U. Pasaogullari, C. Y. Wang, *J. Electrochem. Soc.*, 151 (2004) A399.
24. J. Benziger, J. Nehlsen, D. Blackwell, T. Brennan, J. Itescu, *J. Membr. Sci.*, 261 (2005) 98.
25. A.B. Béléké, K. Miyatake, H. Uchida, M. Watanabe, *Electrochim. Acta*, 53 (2007) 1972.
26. K. Takada, Y. Ishigami, S. Hirakata, M. Uchida, Y. Nagumo, J. Inukai, H. Nishide, M. Watanabe, *Electrochemistry*, 79 (2011) 388.
27. C. Han, I.-T. Kim, H.-J. Sun, G. Park, J.-J. Lee, H.-K. Lee, J. Shim, *Int. J. Electrochem. Sci.*, 7 (2012) 8627.
28. H. Oh, J. Park, K. Min, E. Lee, J.-Y. Jyoung, *Appl. Energy*, 149 (2015) 186.
29. M. Watanabe, M. Tomikawa, S. Motoo, *J. Electroanal. Chem.*, 195 (1985) 81.
30. M. Watanabe, K. Makita, H. Usami, S. Motoo, *J. Electroanal. Chem.*, 197 (1986) 195.
31. M. Giordano, E. Passalacqua, V. Recupero, M. Vivaldi, E. J. Taylor, G. Wilemski, *Electrochim. Acta*, 35 (1990) 1411.
32. J.-C. Shim, S.-H. Ahn, D.-Y. Yoo, J.-S. Lee, *J. Kor. Ind. & Eng. Chem.*, 9 (1998) 89.
33. T. Kenjo, *Denki Kagaku*, 53 (1985) 957.
34. T. Kenjo, K. Kawatsu, *Electrochim. Acta*, 30 (1985) 229.
35. J.-P. Shim, H.-K. Lee, S.-G. Park, J.-S. Lee, *Synthetic Metals*, 71 (1995) 2261.
36. J.-P. Shim, Y.-S. Park, H.-K. Lee, J.-S. Lee, *J. Power Sources*, 74 (1998) 151.
37. T. Sakai, H. Takenaka, E. Torikai, *J. Electrochem. Soc.*, 133 (1986) 88.
38. M. Uchida, Y. Aoyama, N. Eda, A. Ohta, *J. Electrochem. Soc.*, 142 (1995) 4143.
39. N. Miyagawa, H. Igarashi, P. Stonehart, M. Watanabe, 35th Battery Symposium in Japan, p275, Nagoya (1994).
40. K. Konoshita, "Carbon - Electrochemical and Physicochemical Properties", p46, John Wiley & Sons (1988).
41. N. Hara, K. Tsurumi, M. Watanabe, *J. Electroanal. Chem.*, 413 (1996) 81.

42. T.A. Zawodzinski, C. Derouin, S. Radzinski, R.J. Sherman, V.T. Smith, T.E. Springer, S. Gottesfeld, *J. Electrochem. Soc.*, 140 (1993) 1041.
43. K.K. Pushpa, D. Nandan, R. M. Iyer, *J. Chem. Soc. Faraday I*, 84 (1988) 2047.
44. T.A. Zawodzinski, S. Gottesfeld, S. Shoichet, T.J. McCarthy, *J. Appl. Electrochem.*, 23 (1993) 86.
45. A.S. Arico, V. Antonucci, V. Alderucci, E. Modica, N. Giordano, *J. Appl. Electrochem.*, 23 (1993) 1107.
46. T. Kenjo, *Electrochim. Acta*, 31 (1986) 1617.
47. G.-M. Huang, M.-H. Chang, *Int. J. Electrochem. Sci.*, 9 (2014) 7819.
48. C.-T. Liu, M.-H. Chang, *Int. J. Electrochem. Sci.*, 8 (2013) 3687.

© 2015 The Authors. Published by ESG (www.electrochemsci.org). This article is an open access article distributed under the terms and conditions of the Creative Commons Attribution license (<http://creativecommons.org/licenses/by/4.0/>).